Magnetic Shield Design Modeling and Validation for SWOT Spacecraft Ka-band Extended Interaction Klystron

Edward Gonzales, Edward.C.Gonzales@jpl.nasa.gov
Dalia Mcwatters, Dalia.A.Mcwatters@jpl.nasa.gov
Jet Propulsion Laboratory, California Institute of Technology
Pasadena, California

***Abstract*— Two Extended Interaction Klystrons (EIKs) containing strong permanent magnets were modeled magnetically in a representative spacecraft geometry using commercial finite element modeling techniques and were validated against measurements made at varying distances. Initial modeling results for the 63 A-m^2 dipole moment magnets showed that magnetic shields would be necessary in order to meet magnetic field requirements for the Surface Water and Ocean Topography (SWOT) spacecraft, which contains components that are susceptible to external DC magnetic fields. JPL and the EIK vendor proposed cold rolled steel and mu-metal as potential shield materials along with proposed thicknesses of 0.5 mm and 1.5 mm. Magnetic shields made from each of these materials were designed and modeled in software, taking high-field saturation into account. Prototype magnetic shields with these parameters were then built, measured with an existing EIK, and compared against modeling results. For single-axis field measurements along the dipole axis, modeling results were within 7 gauss of the measured values at 10 cm from the magnet, and converged to less than 1.5 gauss at distances greater than 14 cm from the magnet. Three-axis field measurements at locations of interest showed that model correlation improved to within 4 gauss at 11 cm and 2 gauss for distances ranging between 15 cm and 36 cm.**

I. Introduction

The Surface Water Ocean Topography (SWOT) spacecraft is a joint mission between NASA JPL and CNES scheduled to launch in 2020 [1]. The primary science objective is to map the height of earth surface water features to an unprecedented accuracy of 0.8 cm and resolution of 4 km^2 [2]. The primary instrument on SWOT is the Ka-band Radar Interferometer (KaRIn). The KaRIn radar transmitter utilizes an Extended Interaction Klystron (EIK) to amplify the modulated RF pulses. For reliability reasons, a spare EIK is included in the radar design. The EIKs were provided by Communications & Power Industries (CPI) as a contribution to SWOT from the Canadian Space Agency.

EIKs amplify RF signals by modulating a signal onto a focused electron beam. A large permanent magnet is required to focus the electron beam along the length of the EIK. The permanent magnets in the EIK have a magnetic dipole moment of 63 A-m^2 (manufacturer provided value), which at the surface of the magnet can register field strengths up to 1 T. The magnet is a hollow cylinder with radial polarization (South at center, North at outer edge). This provides a magnetic dipole moment along the EIK beam axis (cylinder *z*-axis).

Numerous components on the SWOT spacecraft are sensitive to magnetic fields, including RF components (ferrites, isolators, circulators) and magnetometers for attitude control. Elevated field levels may magnetically saturate these components, thus impairing the function of sensitive scientific instruments and the spacecraft attitude control system (ACS). As a first line of defense, in order to reduce the field strengths on neighboring electronics, the two EIKs were oriented opposite to each other to profit from some field cancellation. Orientation alone is insufficient to control the spacecraft magnetic environment, so magnetic shielding of the EIKs will be also required. Various shielding options were proposed by CPI and JPL engineers. Mu-metal and cold-rolled steel were proposed as shielding materials. Proposed shield thicknesses for either material were 0.5 mm and 1.5 mm.

Quantified values for shielding effectiveness across these variables were previously unavailable. Additionally, spacecraft subsystem engineers wanted to understand the magnetic environment at their individual locations in order to evaluate the risk to their performance. To address these concerns, computational magnetic modeling methods were used to evaluate the most appropriate shield material and thickness. In order to validate the computer simulation, prototype shields of each material were designed, built, and measured on a representative EIK.

Previous modeling efforts at JPL explored the effect of EIK orientation on the spacecraft magnetic environment [3]. However, magnetic sources in this modeling activity were not calibrated to a real magnetic source and were only used for comparative studies between different EIK configurations. Accurate shielding was also not considered. This paper describes a modeling method that addresses both concerns while also building on the heritage of previous modeling activities.

II. Modeling and Calibration

The large permanent magnets in the EIK were modeled magnetostatically using ANSYS Maxwell modeling software. Maxwell operates by dividing a three dimensional geometry into a “mesh” of small tetrahedral units within which

Maxwell's Equations are solved. An initial guess (or solution "pass") for the distribution of tetrahedrons is solved and a figure of merit for the solution ("energy") is generated. In subsequent passes, tetrahedrons are added to the mesh until the percent-delta in energy between passes converges to a user-provided value. The user typically specifies at least the maximum number of passes (default = 10) and a required minimum percent delta (default = 1%). Default solution parameters were used in this activity for models where shield saturation was not considered.

The EIK magnets were modeled as coils of wire driven by a large current (Fig. 1). Modeling the magnets as wire coils instead of magnetic materials enabled calibration of the moment using intuitive parameters (drive current and coil area) correlated to the known approximate magnetic moment of the actual magnets. Selecting the drive coil parameters involved first-order calculations with further refinement by measurement. Coil size was selected such that it represented a volume on the order of the actual magnet. From a known area and magnetic moment, an estimated drive current could be calculated. However, since the coil had a non-zero thickness, the actual moment varied slightly but provided a value on the correct order of magnitude. Further refinement of the magnetic moment would be achieved by varying drive current to match measured values.

An engineering model EIK with magnetic properties comparable to the SWOT EIK was measured for model calibration. The magnet is located along one of the walls of the unit. Taking this wall to be z = 0, measurements were taken at various distances along the axis through the center of the magnet with a Lakeshore 475 gaussmeter and axial probe. The axial component of the magnetic field vector was assumed the dominant field component; transverse/radial field components were not recorded for measurements taken along the magnet dipole axis. Spot checks of transverse fields were taken and confirmed this assumption. Measurements were taken at the nearest possible distance to the EIK (z = ~8 cm due to flanges and wire-exits) through z = ~100 cm (Fig. 2). (Metric values are approximate as measurements were taken in inches and subsequently converted to centimeters.) Although measurements were taken out to 100 cm for completeness, the measured values approached the background level of the Earth magnetic field beyond 50 cm.

Drive current was modified iteratively from original estimates such that simulated values closely matched measured values (Fig. 3). The simulated and measured values for magnetic field follow a similar $1/r^3$ fall-off, indicating that the simulated location of the wire coil and assumed behavior of the magnetic moment were representative of the EIK magnet. Once drive current was set for the no-shield case, it was not adjusted in subsequent simulations.

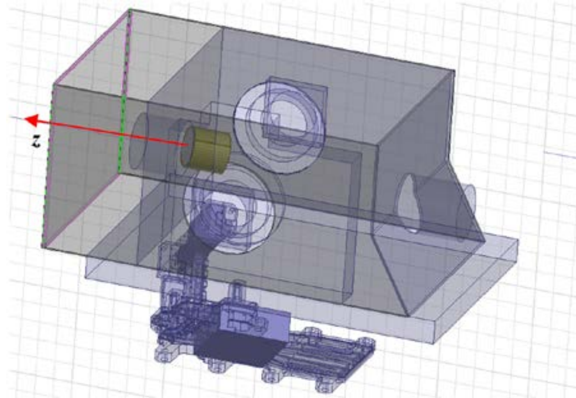

Fig. 1. EIK model with conformal shield

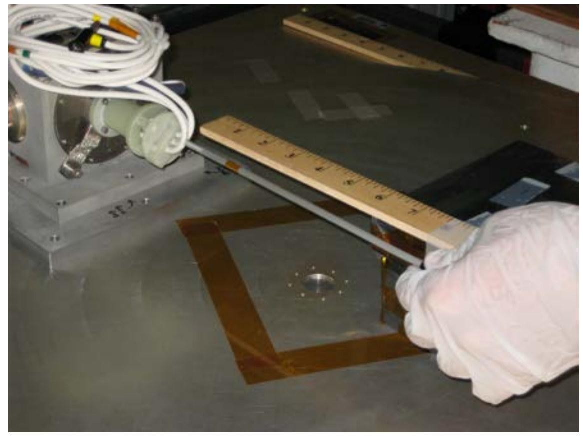

Fig. 2. Measuring EIK without shield, axial component

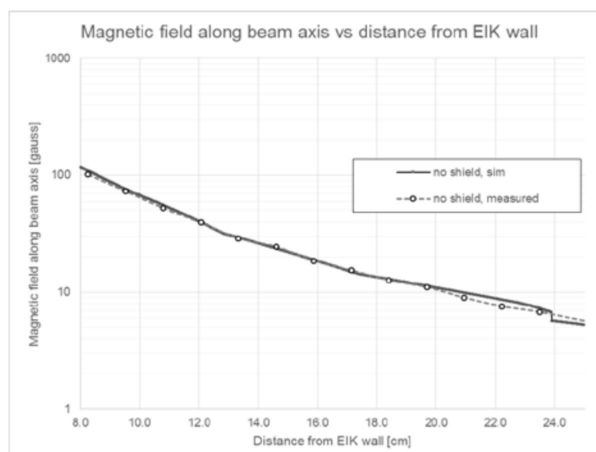

Fig. 3. Magnetic field [gauss] vs. distance [cm], no-shield simulated and measured, axial component only

III. Prototype Shield Modeling and Testing

After the magnetic model was validated for the baseline "no shield" condition, magnetic shields were designed, simulated, and built. Two types of shields were designed: an open-topped box (Fig. 4); and a shield that conformed to the contours of the EIK (Fig. 1). The open-topped box was designed so that it could be built with standard metal-shop tools and would be robust to mechanical uncertainties. The conformal shield would be more difficult to manufacture but is more representative of what would ultimately be built for the flight EIKs. For the purposes of this simulation and validation, the open-topped box was sufficient.

The open-topped box was designed to be open along one edge so that it could be removed easily. A 5 mm lip was added to the open end so that the edges overlapped and ensured continuity of the magnetic field. For the purposes of modeling, the open-topped box was modeled without the lip.

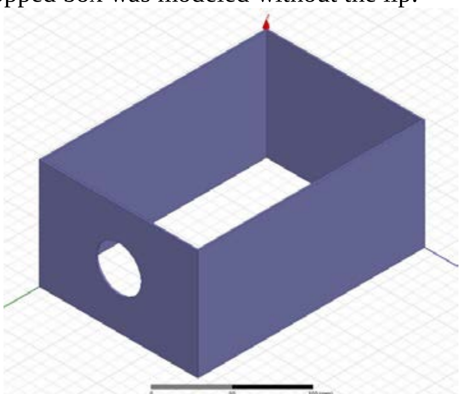

Fig. 4. Open-topped shield design

A. *Modifications to default simulation parameters*

In order to model material magnetic effects correctly, two modifications to the default simulation parameters were required: a modified material B-H curve for mu-metal and a decrease in solution nonlinear residual. Maxwell has a library of standard materials and their properties, including permeability. Permeability can be specified as a B-H curve. However, the B-H curve for mu-metal was insufficiently specified at the high H-field levels observed, leading to possible errors when extrapolating values. The level to which these field levels needed to be specified can be estimated by measurements of the EIK in free-space. At points very near the magnet (approximating the distance of the shield), measured fields were on the order of 0.5 T corresponding to $|\mathbf{H}| = 4.0 \times 10^5$ A/m. Therefore, the mu-metal curve was manually extended from the ~3000 A/m in the standard library to 280 000 A/m, which was sufficient to accurately extrapolate for any **H** beyond it (Fig. 5).

Nonlinear residual is a solution setting in Maxwell that specifies the precision of the nonlinear operating point i.e. where the simulation operates along a material's B-H curve at any given point in space. Default simulation settings specify non-linear residual at 1.0×10^{-3} (unitless). In order to model saturation with sufficient precision, nonlinear residual needed to be significantly smaller. 1.0×10^{-7} was ultimately used per suggestion from ANSYS application engineers. All other solution parameters were left at their default settings.

Prior to the application of the above modifications, initial simulations showed anomalous results. For example, mu-metal performance could vary wildly between runs, and 0.5 mm 1010 cold rolled steel was only marginally better than having no shield at all. After the modifications, simulation results were more stable across runs and showed a trend that aligned better with intuition. The effect of each modification taken individually was not quantified.

Once the modeling parameters were stabilized, actual shields were built to validate the performance of steel vs. mu-metal at various thicknesses. The exact combinations of requested thickness and material were not readily available, so suitable replacements were used. Cold rolled steel 1010 in 0.43 mm (17 mils) and 1.58 mm (63 mils) were available, as well as mu-metal in 0.64 mm (25 mils). The discrepancies in material thickness compared to the requested/simulated values was considered small to a first order. Sufficiently thick mu-metal was not available at the time of the test, so instead a double layer of 0.64 mm mu-metal was simulated and tested. As in the case without shields, measurements were taken along the *z*-axis of the magnet dipole between ~8 cm to ~100 cm. Manufactured shields and placement on the EIK are shown in Fig. 6 and Fig. 7.

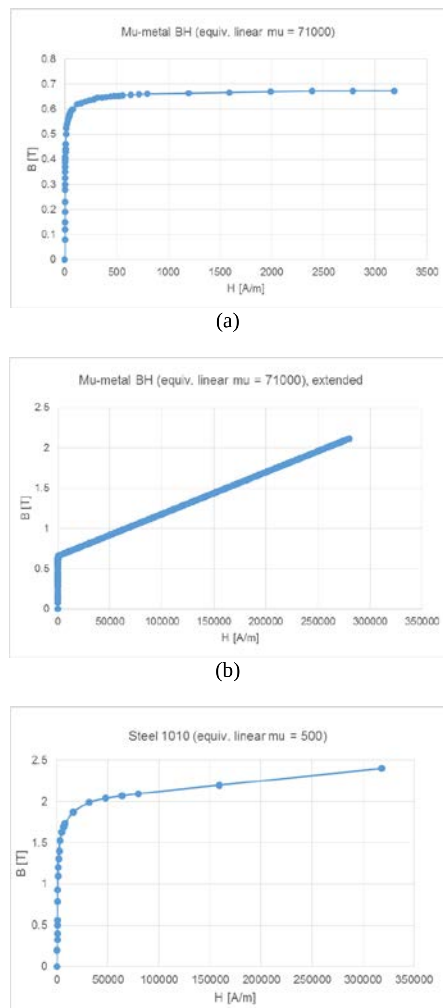

(a)

(b)

(c)

Fig. 5. B-H curves for shield materials: (a) mu-metal, (b) mu-metal extended to $H = 2.8 \times 10^5$ A/m. (c) cold rolled steel 1010

Fig. 6. Built open-topped shield, 1010 cold rolled steel, 0.43 mm

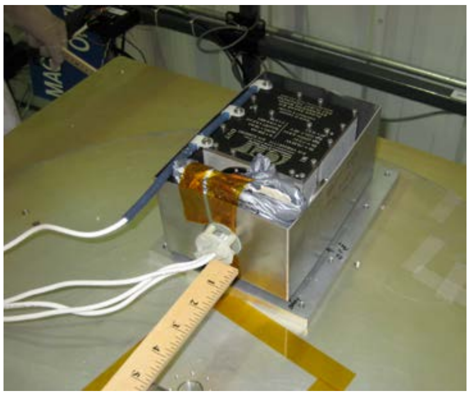

Fig. 7. EIK with 1.58 mm steel shield

B. *Measurements at points of interest*

In addition to on-axis data, measurements were also taken at off-axis locations emulating spacecraft locations of interest. Since only one EIK was available to measure, a simulation was run with one EIK's magnet "turned off."

When measuring the field at a point of interest, a commonly-accepted method for evaluating simulated field levels at point-locations was used [4][5]. A fictitious sphere with a volume on the order of how accurately the measurement probe could be placed by hand (assumed r_{sph} = 20 mm) was placed at the location of interest within the Maxwell model. The field was then volume-averaged in the software according to the equation:

$$|\mathbf{B}_{avg,V}| = \frac{\iiint_V |\mathbf{B}(x,y,z)| dv}{\iiint_V dv}$$

where **B**(x,y,z) is the field at a given point within the solution volume V.

Since the magnetic field off-axis contains both axial and radial components, a three-axis gaussmeter was required. Measurements at these points of interest were taken using an AlphaLab VGM three-axis gaussmeter and adjusted for the background magnetic field of the Earth.

IV. Test Results

A. *On Axis*

On-axis measurement results between 8 and 24 cm are shown in Fig. 8. Nominal material thicknesses are referenced in the legend (e.g. 0.5 mm intended thickness instead of 0.43 mm actual). Solid lines indicate simulated values and dashed lines with discrete points are measured values. Error associated with shielding materials is shown in Fig. 9.

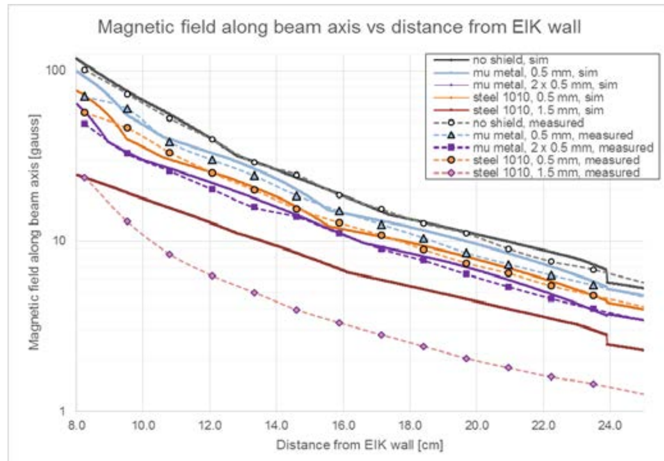

Fig. 8. On-axis measurement results, axial component only

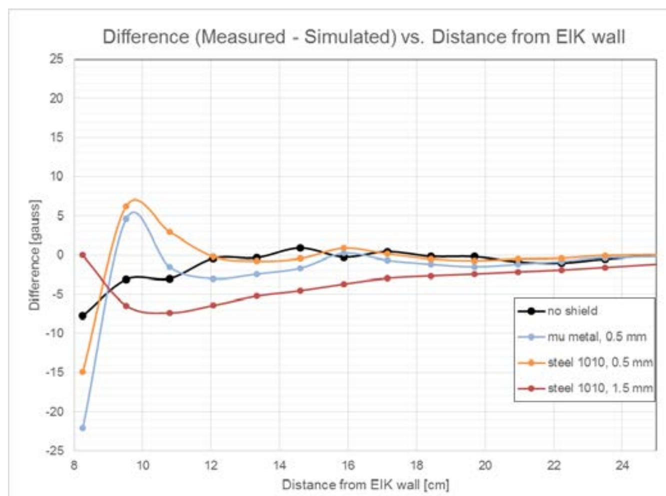

Fig. 9. Difference [gauss] vs. distance from EIK wall [cm]. Mu-metal 2 x 0.5 mm not shown

B. *Off-Axis (Points of interest)*

Table I shows the three-axis magnetic field measurements at five locations of interest at distances varying between 107 mm and 798 mm from the EIK magnet at varying azimuth and elevation from the dipole axis.

TABLE I
COMPARISON OF SIMULATED AND MEASURED MAGNETIC FIELDS AT OFF-AXIS POINTS OF INTEREST

	Distance to magnet [mm]	0.5 mm steel shield			1.5 mm steel shield		
		B (sim) [gauss]	B (meas) [gauss]	Diff [gauss]	B (sim) [gauss]	B (meas) [gauss]	Diff [gauss]
Location 1	107	12.71	8.84	-3.87	5.54	1.48	-4.06
Location 2	158	2.36	1.30	-1.06	1.22	0.28	-0.94
Location 3	389	6.40	7.55	1.15	2.89	2.17	-0.72
Location 4	356	2.19	3.85	1.66	1.08	0.22	-0.86
Location 5	798	0.10	-0.24	-0.34	0.04	-0.45	-0.49

V. Error Accounting

On-axis measured values very closely matched simulated values as well as the trend vs. distance across all materials and thicknesses. More error can be observed in the steel 1010 case but is amplified by the log-log scale: error in this case is on the order of single digit gauss and converges to a constant scaling factor offset (decreasing linear error) beyond 12 cm.

The greatest magnitude error for single-axis measurements occurs at distances within 10 cm of the EIK magnet. This is likely attributed to the complex nature of field vectors close to the shield. At these distances, the assumption that the magnetic field consists primarily of a single vector component is not valid. Use of a three-axis gaussmeter can mitigate these issues but was not measured here. At distances greater than 10 cm, most measurements were well within 7 gauss and improved with distance from the EIK wall.

Similar trends can be observed for the three-axis measurements at points of interest. The 1.5 mm steel shield has larger error compared to the 0.5 mm shield but converges to small error at larger distances. Locations at close range and far off-axis exhibit correlation to within 4 gauss in all cases—such as Location 2 in Table I, which lies 15.8 cm from the magnet and approximately 60 degrees off-axis.

While probe positional error was pervasive in all measurements, it was especially challenging in the three-axis measurements as probe location was significantly less controlled. The probe was located in three-dimensional space relative to the EIK with only the use of meter sticks. This method was prone to error, but all efforts were made to ensure accurate placement.

VI. Summary

Challenges in controlling the magnetic environment of the SWOT spacecraft necessitated the use of finite element modeling methods. Modeling was not without its own challenges due to the material behavior in a very high magnetic field environment. However, with close attention paid to simulation nuances, material behavior, and model calibration using measured data, results from modeling methods were found to correlate very well with measurement. Good correlation was observed across multiple measurement methods and tools, lending further credibility to the simulation results. Additionally, sources of error are well understood.

Such confidence in the modeling results has helped guide several design decisions in the SWOT spacecraft. Among these design decisions was the selection of 1.5 mm steel as the EIK shielding material. Additionally, modeling different design iterations played a significant role in determining the size and shape of the flight EIK shields. The location of the EIKs within the spacecraft and the placement of electronics relative to them have also benefited from these magnetic modeling efforts.

Given the results of this validation, future efforts by the authors in understanding spacecraft magnetic field environment will likely employ an increasing use of finite element modeling methods.

Acknowledgment

N. Huang provided the original EIK magnetic model and assistance in interpreting it.

P. Narvaez and W. Hatch from the JPL EMC Group provided guidance in the modeling and test activities.

C. Rhoades from the JPL EMC Group assisted in taking magnetic measurements.

Dr. J. Saitz from ANSYS provided insight into modeling saturation effects and correlating simulation to measurement.

The work described in this paper was carried out at the Jet Propulsion Laboratory, California Institute of Technology, under a contract with the National Aeronautics and Space Administration.

COPYRIGHT

REFERENCES

[1] SWOT Launch Date, https://swot.jpl.nasa.gov/news/index.cfm?FuseAction=ShowNews&NewsID=23 (accessed April 22, 2016)

[2] SWOT: Science, http://swot.jpl.nasa.gov/science/ (accessed April 22, 2016)

[3] N. Huang, "SWOT EIK Initial Magnetic Modeling Results," Jet Propulsion Laboratory, Pasadena, CA, USA, IOM 5132-14-002, Jan. 2014

[4] Testing Electromagnetic Analysis Methods (T.E.A.M.), http://www.compumag.org/jsite/team.html (accessed April 25, 2016)

[5] J. Saitz, private communication, Feb. 2016

BIOGRAPHIES

Edward Gonzales is an EMC engineer working on SWOT and is co-lead EMC Engineer for the Mars 2020 Rover. He also provides support for the Europa Clipper Mission.

Dalia Mcwatters (at JPL since 1985) is the Instrument Engineer for the Surface Water Ocean Topography mission's prime instrument: the Ka-band Radar Interferometer. Her previous earth science space instruments include Aquarius which measured sea-surface salinity from the Argentinean SAC-D spacecraft during 2011-2014, and the Shuttle Radar Topography Mission which produced a high resolution land height map over 11 days of the STS-99 Endeavor mission.